Numerical analysis of degradation processes in laminated composite materials

M.H.J.W. PAAS and J. VAN DEN EIKHOFF
Centre for Mechanical Engineering
TNO Building and Construction Research

Abstract

Progressive failure in fiber-reinforced composite materials is modeled using continuum damage mechanics. The anisotropy in the damage is accounted for by a second order tensor. Constitutive equations for the stress tensor and the damage evolution tensor in conjunction with a damage growth criterion are provided. The numerical procedures for solving the governing equations are presented. A comparison with available experimental results on uniaxial loading of a graphite-epoxy $[0/90_2]_s$ laminate shows good agreement. Bending of a laminated composite structure is simulated. The influence of the finite element discretization on the results is investigated.

Keywords. Continuum damage mechanics, laminated composites, finite element analysis.

1. Introduction

The increased use of laminated fiber-reinforced composite materials in structural applications necessitates a thorough understanding of their behavior under various loading conditions. In particular the trend toward higher design levels has led to the need to understand failure initiation and to predict strength. The modeling of progressive failure of laminated composites is usually based on the application of strength criteria to check whether ply failure has occurred (Nahas 1986, Chang et al. 1991). If such is the case the material stiffness matrix is modified to account for the loss in stiffness. In this approach the degradation process is governed by a sequence of instantaneous ply failures. A continuum damage model for brittle deformation processes in solid materials subjected to quasistatic and fatigue loadings has been proposed by Paas and van den Eikhoff (1992, 1993). The anisotropy in the damage is accounted for by a symmetric second order tensor. The model is derived on a thermodynamical basis and is suited for large deformations. Constitutive equations are required for: (1) the stress-strain relation of the damaged continuum, (2) the damage growth law and (3) a criterion for damage growth. In this paper the damage model is adopted to describe the degradation of laminated composite structures subjected to quasistatic loadings. The typical stages in laminate failure are assessed. The numerical procedures for solving the governing equations are presented. Emphasis is placed on the determination of the finite element equations, the damage, the damage surface, the tangential stiffness matrix and the application of arc-length control to pass the limit point in the load-displacement curves. Example applications, showing the response of laminated structures to monotonic loadings, are presented. The influence of mesh refinement on the finite element analyses is investigated.

2. Damage characterization

Consider a volume element containing many microcracks, that are distributed in a statistically homogeneous manner. Since the shapes of the cracks in this representative volume element (RVE) are generally unknown, they may be approximated by some equivalent flat surfaces. The restriction to brittle material response implies that the energy dissipated is the result of crack growth only and that crack growth is governed by cleavage 1 (Krajcinovic 1989). Then a natural choice is to assign to each equivalent flat crack a vector $\vec{d}$, whose magnitude is a function of the crack surface A and a characteristic crack dimension a, and whose direction is normal to the crack plane. Thus, we have for the k^{th} crack

$$\vec{d}_k = d_k \vec{n}_k \quad ; \quad d_k = f(A_k, a_k) \tag{1}$$

Since each crack possesses two equal and opposite surfaces, the description should be independent of the sense of the normal $\vec{n}_k$. This is accomplished by representing the microcrack by a dyadic vector product $\vec{d}_k \otimes \vec{d}_k$. If the damage entities are sparsely dispersed and therefore non-interactive, the total representation of all N cracks in the RVE can be constructed by summation. Then the damage state is characterized by a symmetric second order tensor

$$\boldsymbol{D} = \frac{1}{\Delta^2} \sum_{k=1}^{N} \vec{d}_k \otimes \vec{d}_k \tag{2}$$

where Δ is a material parameter, such that the damage tensor is a dimensionless quantity. A special form of (2) was employed by Weitsman (1988a, 1988b), who used $d_k = A_k$ and Δ as the area of anyone of the sides of the RVE.

3. Constitutive theory

During an irreversible thermodynamic process, the elastic strain and stress are insufficient to describe the state of the material locally. The changes in the microstructure must be defined by an additional set of internal variables. Under the assumption that microcrack growth is the dominant mode of microstructural changes, an internal variable $\boldsymbol{D}$ characterizing the damage is introduced. Under isothermal conditions application of the Clausius-Duhem inequality yields that the stress-strain relation for linear elastic material can be expressed as

$$\sigma = {}^4\boldsymbol{C}(\boldsymbol{D}) : \varepsilon \tag{3}$$

In addition, the damage rate tensor must obey

$$\boldsymbol{X} : \dot{\boldsymbol{D}} \geq 0 \tag{4}$$

where $\boldsymbol{X}$ is the thermodynamic force conjugate to the thermodynamic flux $\dot{\boldsymbol{D}}$

$$X = -\tfrac{1}{2}\varepsilon : \frac{\partial\,^4\boldsymbol{C}}{\partial \boldsymbol{D}} : \varepsilon \tag{5}$$

The thermodynamic force can alternatively be written in a stress-based form

$$X = \tfrac{1}{2}\sigma : \frac{\partial\,^4\boldsymbol{S}}{\partial \boldsymbol{D}} : \sigma \tag{6}$$

with $^4\boldsymbol{S}$ the compliance tensor.

A criterion for damage growth is established by proposing the existence of a closed domain Ω in the thermodynamic force space, which contains the origin and which is bounded by the surface Γ. The damage surface is a piecewise smooth and convex surface enveloping the locus of all points in the space of thermodynamic forces which can be reached without change in the current state. Let the damage kinetics be governed by m modes, where each mode refers to an ensemble of cracks with identical geometrical features. The reversible domain Ω is defined as

$$\Omega = \bigcap_{\alpha=1}^{m} \Omega_\alpha \quad ; \quad \Omega_\alpha = \{\, X \in \mathbb{R}^6 \mid \phi_\alpha(X, \nu_\alpha) < 0 \,\} \tag{7}$$

where ϕ_α is a dissipation potential and ν_α is a history dependent parameter, which determines the current location of the damage surface for mode α in the space of thermodynamic forces. Invoking the normality rule (Malvern 1969) the rate of change of the damage for mode α is given by

$$\dot{\boldsymbol{D}}^{(\alpha)} = \lambda_\alpha \frac{\partial \phi_\alpha}{\partial X} \tag{8}$$

with λ_α a nonnegative multiplier. It can be verified easily that (8) satisfies the Clausius-Duhem inequality for convex ϕ_α. The conditions for damage growth are formulated as

$$\phi_\alpha \le 0 \ ; \ \lambda_\alpha \ge 0 \ ; \ \lambda_\alpha \phi_\alpha = 0 \tag{9}$$

In case of damage growth, the current damage surface is determined from the consistency condition

$$\dot{\phi}_\alpha = 0 \ \Rightarrow \ \dot{\nu}_\alpha = -\left(\frac{\partial \phi_\alpha}{\partial \nu_\alpha}\right)^{-1} \frac{\partial \phi_\alpha}{\partial X} : \langle \dot{X} \rangle \tag{10}$$

where $\langle\cdot\rangle$ denotes the McAuley brackets. In brittle processes, the current state may not depend upon the rate at which this state has been realized. This leads to defining (Paas and van den Eikhoff 1992)

$$\lambda_\alpha = \dot{\nu}_\alpha \tag{11}$$

4. Damage assessment in composite laminates

Progressive failure of multilayered composite laminates exhibits some typical stages. During loading the first detectable damage is cracking of the matrix in the off-axis plies. These cracks are triggered by microdefects and propagate along the fibers. As with increasing load levels more cracks develop, the in-between tensile stresses diminish, such that cracks continue to occur at a diminishing rate until a crack saturation density is achieved. This crack saturation density is commonly referred to as the characteristic damage state (Reifsnider and Giacco 1990). With continued loading, subsequent damage consists of initiation of cracks transverse to the primary cracks in adjacent layers. At locations, where cracks of two adjacent plies cross there is a highly three-dimensional local stress state which can cause fiber fracture and local delaminations. Further increase in damage is highly localized and involves large scale fiber failures. The final failure event is determined by the formation of a failure path through the locally failed regions and is therefore highly stochastic.

The damage model will be used to predict failure of composite laminates. In general, the initial material symmetry in the plies is removed even for low damage densities of one orientation (Talreja 1990). Orthotropy is only retained when the defect directions coincide with the mutually orthogonal axes of symmetry $\vec{n}_1$, $\vec{n}_2$, $\vec{n}_3$, with the subscripts 1, 2 and 3 designating the fiber direction, the transverse direction and the normal direction in a laminate ply. In this particular case the damage tensor takes the form

$$D = \sum_{\alpha=1}^{3} D^{(\alpha)} \quad ; \quad D^{(\alpha)} = D_\alpha \vec{n}_\alpha \otimes \vec{n}_\alpha \tag{12}$$

with α = 1, 2, 3 denoting fiber fracture, matrix cracking and delamination respectively. In what follows we restrict attention to fiber fracture and transverse matrix cracking.

Stress-strain relation

The stress-strain relation is influenced by the existence of transverse matrix cracks and fiber breaks. The effects of regular arrays of transverse matrix cracks on the stress-strain behavior have been established by Laws et al. (1983), who employed a self consistent method. This approach was used by Paas and van den Eikhoff (1992, 1993) to calculate the compliances S_{22} and S_{66} for varying matrix crack densities. These compliances were fitted by exponential functions with best-fit coefficients γ_{22} and γ_{66}. The effects of fiber fracture are accounted for by assuming that S_{11} and S_{66} are inversely proportional to the density of broken fibers ($0 \leq D_1 < 1$). Hence, the damage induced compliances for a unidirectional reinforced ply are approximated as

$$[S] = \begin{bmatrix} \dfrac{1}{E_{11}^{0}(1-D_1)} & -\dfrac{\nu_{12}^{0}}{E_{11}} & 0 \\ -\dfrac{\nu_{12}^{0}}{E_{11}} & \dfrac{\exp(\gamma_{22}D_2)}{E_{22}^{0}} & 0 \\ 0 & 0 & \dfrac{\exp(\gamma_{66}D_2)}{2G_{12}^{0}(1-D_1)} \end{bmatrix} \tag{13}$$

Damage evolution
In composite laminates the defect directions are channeled by the presence of fibers and adjacent plies, such that the damage modes are not prone to directional changes. From (8) the damage rate can be written as

$$\dot{\boldsymbol{D}}^{(\alpha)} = \sum_{i=1}^{3} \lambda_{\alpha} \frac{\partial \phi_{\alpha}}{\partial X_i} \vec{n}_i \otimes \vec{n}_i \tag{14}$$

The requirement that the initial defect directions do not change, necessarily involves that the dissipation potential ϕ_α may only depend on X_α, yielding

$$\dot{\boldsymbol{D}} = \sum_{\alpha=1}^{3} \dot{\boldsymbol{D}}^{(\alpha)} \quad ; \quad \dot{\boldsymbol{D}}^{(\alpha)} = \lambda_{\alpha} \frac{\partial \phi_{\alpha}}{\partial X_{\alpha}} \vec{n}_{\alpha} \otimes \vec{n}_{\alpha} \tag{15}$$

Using (6) and (13) the thermodynamic force associated with fiber fracture is

$$X_1 = \frac{1}{(1-D_1)^2} \frac{\sigma_{11}^2}{2E_{11}^{0}} + \frac{\exp(\gamma_{66}D_2)}{(1-D_1)^2} \frac{\sigma_{21}^2}{4G_{12}^{0}} \tag{16}$$

and the thermodynamic force associated with transverse matrix cracking is

$$X_2 = \exp(\gamma_{22}D_2) \frac{\gamma_{22}\langle\sigma_{22}\rangle^2}{2E_{22}^{0}} + \exp(\gamma_{66}D_2) \frac{\gamma_{66}\sigma_{21}^2}{4G_{12}^{0}} \tag{17}$$

The McAuley brackets in (17) account for the fact that a compressive transverse stress will close the existing transverse cracks.

Damage growth in mode α occurs when the associated thermodynamic force exceeds a critical value. This is accomplished by choosing the dissipation potential as a linear function of the thermodynamic forces

$$\phi_{\alpha} = A_{\alpha}[X_{\alpha} - \nu_{\alpha} X_{\alpha}^{o}] \tag{18}$$

with A_α a positive constant. From (16) and (17) it follows that $\phi_\alpha = 0$ ($\alpha = 1,2$) is an ellipse in stress space. This result is in accordance with fracture mechanics concepts (Paas and van den Eikhoff 1992, 1993). It is remarked that quadratic stress-based strength criteria have also found widespread use as macroscopic failure criteria for laminates (Nahas 1986). Using (8)-(11) and (18) the damage is derived as

$$D_\alpha = D_\alpha^0 + A_\alpha(\nu_\alpha - 1) \quad ; \quad \nu_\alpha = \max_{0<\tau<t}\left[1, \frac{X_\alpha(\tau)}{X_\alpha^0}\right] \tag{19}$$

A similar relation for the damage has been advocated by Allix and Ladeveze (1989), who obtained a linear relationship between the damage variables and the associated thermodynamic forces based on experimental observations. However, the expressions for the thermodynamic forces as proposed by Allix and Ladeveze differ from the ones used in this paper.

5. Numerical procedures

Since dissipative mechanisms take place, a particular analysis includes path dependent phenomena. Throughout the complete history of load application, equilibrium must be satisfied. The loading history is applied in increments. In each loading increment the displacement field and the damage must be determined. The model has been implemented in the DIANA finite element package. In the following the numerical procedures for solving the governing equations are discussed.

Weighted residuals formulation

According to the principle of weighted residuals the equilibrium equation (inertial forces and body forces are omitted) is equivalent to the requirement that at every instant and for all admissible weighting functions $\vec{w}$, the following integral equation is satisfied (Bathe 1982)

$$\int_V \vec{w}\cdot(\nabla\cdot\sigma)\,dV = 0 \tag{20}$$

where ∇ is the gradient operator and V is the current volume of the body. Using integration by parts and Gauss' theorem, the weak form of the principle of weighted residuals is obtained

$$\int_V (\nabla\vec{w})^T : \sigma\,dV = \int_A \vec{w}\cdot\vec{t}\,dA \tag{21}$$

where $\vec{t} = \sigma\cdot\vec{n}$ is the external force vector on the surface A. An estimate for the displacements at time $t+\Delta t$ is given by

$$\vec{u}_n = \vec{u}_o + \delta\vec{u} \tag{22}$$

with the subscript n meaning new and o meaning old and with δ denoting an iterative change. Using the strain-displacement relation

$$\varepsilon = \tfrac{1}{2}\left((\nabla\vec{u}) + (\nabla\vec{u})^T\right) \tag{23}$$

the weighted residuals form becomes

$$\int_V (\nabla\vec{w})^T : {}^4\boldsymbol{C}^{ED} : \delta\varepsilon \, dV = -\int_V (\nabla\vec{w})^T : \sigma \, dV + \int_A \vec{w} \cdot \vec{t} dA \tag{24}$$

where ${}^4\boldsymbol{C}^{ED}$ is the elastic-damage incremental stress-strain tensor.

In order to characterize the response of multilayered laminates, it is necessary to globally average the local ply constitutive equations. This can be established using classical lamination theory (Jones 1975), which is based on the Kirchhoff hypothesis in linear plate theory. In Voigt notation the relevant strains in the plies are given by

$$\underline{\varepsilon} = \underline{\varepsilon}_0 + z \, \underline{\kappa} \tag{25}$$

where

$$\underline{\varepsilon}_0 = \left(\frac{\partial u_0}{\partial x} \; \frac{\partial v_0}{\partial y} \; \frac{\partial u_0}{\partial y} + \frac{\partial v_0}{\partial x} \right)^T \quad ; \quad \underline{\kappa} = -\left(\frac{\partial^2 w_0}{\partial x^2} \; \frac{\partial^2 w_0}{\partial y^2} \; 2\frac{\partial^2 w_0}{\partial x \partial y} \right)^T \tag{26}$$

with the subscript $_0$ denoting mid-plane values. Choosing the weighting functions as $\vec{w} = \delta\vec{u}$ the principle of virtual work is obtained

$$\int_V (\delta\underline{\varepsilon}_0 \;\; \delta\underline{\kappa}) \begin{pmatrix} [C] & z[C] \\ z[C] & z^2[C] \end{pmatrix} \begin{pmatrix} \delta\underline{\varepsilon}_0 \\ \delta\underline{\kappa} \end{pmatrix} dV = -\int_V \delta\underline{\varepsilon}^T \underline{\sigma} \, dV + \int_A \delta\underline{u}^T \underline{t} \, dA \tag{27}$$

Finite element equations

After discretization of the position vector field, the strain-displacement relation becomes

$$\begin{pmatrix} \underline{\varepsilon}_0 \\ \underline{\kappa} \end{pmatrix} = \begin{pmatrix} [D_0]\underline{u}_0 \\ [D_1]\underline{\varphi} \end{pmatrix} = \begin{pmatrix} [D_0][\Phi_0] & [0] \\ [0] & [D_1][\Phi_1] \end{pmatrix} \begin{pmatrix} \underline{\tilde{u}}_0 \\ \underline{\tilde{\varphi}}_0 \end{pmatrix} = [B]\underline{a} \tag{28}$$

with ~ denoting nodal point values. The linearized set of equations for the unknown nodal point displacements $\underline{a}$ can be derived as

$$[K(\underline{a}_o)]\delta\underline{a} = -\underline{h}_i(\underline{a}_o) + \mu_n \underline{h}_e \tag{29}$$

In the iterative equation μ_n is a load-level parameter, which scales up the fixed external loading vector $\underline{h}_e$. The stiffness matrix $[K]$ and the internal force vector $\underline{h}_i$ are given by

$$[K] = \sum_{e=1}^{nel} \int_{A^e} [B]^T \begin{pmatrix} [Q_1] & [Q_2] \\ [Q_2] & [Q_3] \end{pmatrix} [B] \, dA \quad ; \quad \underline{h}_i = \sum_{e=1}^{nel} \int_{V^e} [B]^T \underline{\sigma} \, dV \tag{30}$$

The extensional stiffness matrix $[Q_1]$, the coupling stiffness matrix $[Q_2]$ and the bending stiffness matrix $[Q_3]$ in $(30)_1$ are

$$
\begin{aligned}
[Q_1] &= \sum_{l=1}^{N} [C_l^{ED}](z_l - z_{l-1}) \\
[Q_2] &= \frac{1}{2}\sum_{l=1}^{N} [C_l^{ED}](z_l^2 - z_{l-1}^2) \\
[Q_3] &= \frac{1}{3}\sum_{l=1}^{N} [C_l^{ED}](z_l^3 - z_{l-1}^3)
\end{aligned}
\tag{31}
$$

where l denotes the ply number. In what follows we focus on symmetric laminates ($[Q_2] = [0]$), which are subjected to in-plane loadings.

Arc-length control

For increasing damage the load-displacement curve may have a limit point after which softening occurs. In a standard load-control procedure limit points cannot be passed. Thus, for tracing the equilibrium path in case of softening behavior, a method for arc-length control must be used. The main essence of the arc-length methods is that the load parameter becomes a variable which must be solved simultaneously with the displacement variables. The load-level parameter is determined by an additional constraint for the arc-length, which can be written in an incremental form (Crisfield 1991)

$$
\Delta \underline{a}^T \Delta \underline{a} + \Delta\mu^2 \varphi^2 \underline{h}_e^T \underline{h}_e - \Delta r^2 = 0 \tag{32}
$$

where φ is a scaling parameter for the load contribution and Δr is (an approximation to) the incremental arc-length. The iterative displacements $\delta \underline{a}$ are split into two parts

$$
\Delta \underline{a}_n = \Delta \underline{a}_o + \delta \underline{a} \quad ; \quad \delta \underline{a} = \delta \underline{a}^I + \delta\mu \, \delta \underline{a}^{II} \tag{33}
$$

with

$$
\delta \underline{a}^I = -[K]^{-1}(\underline{h}_i(\underline{a}_o) - \mu_o \underline{h}_e) \quad ; \quad \delta \underline{a}^{II} = [K]^{-1} \underline{h}_e \tag{34}
$$

The iterative displacement $\delta \underline{a}^I$ would also stem from a standard load-controlled Newton-Raphson method with fixed μ_o. The new μ_n is found by substituting (33) in (32) and solving the resulting quadratic equation in $\delta\mu$. The arc-length radius in the current increment is determined by a self adaptive scheme (Crisfield 1991)

$$
\Delta r_n = \Delta r_o \sqrt{\frac{I_d}{I_o}} \tag{35}
$$

with I_o the number of iterations in the previous step and I_d the number of desired iterations.

Damage initiation

The loading which results in damage initiation must be determined. Suppose we initially prescribe a small load increment $\underline{h}_e$, such that the structure behaves elastically everywhere.

The determination of the strain vector, that is located on the initial damage surface, consists of computing the factor R, which projects the local strains $\underline{\varepsilon}_e$ on the damage surface. Using (5) and (18) we find

$$R = \sqrt{\frac{X^0}{X(\underline{\varepsilon}_e, \underline{D} = \underline{0})}} \tag{36}$$

Damage and damage surface

Using (15) and (11) the incremental change of damage mode α is

$$\Delta D_\alpha = H(\phi_\alpha) \frac{\partial \phi_\alpha}{\partial X_\alpha} \Delta \nu_\alpha > 0 \tag{37}$$

with $H(\cdot)$ the Heaviside step function. Invoking the consistency condition yields

$$\Delta \phi_\alpha = \frac{\partial \phi_\alpha}{\partial X_\alpha} \Delta X_\alpha + \frac{\partial \phi_\alpha}{\partial \nu_\alpha} \Delta \nu_\alpha = 0 \tag{38}$$

The incremental change in the thermodynamic force is

$$\Delta X_\alpha = \frac{\partial X_\alpha}{\partial \underline{D}}^T \Delta \underline{D} + \frac{\partial X_\alpha}{\partial \underline{\varepsilon}}^T \Delta \underline{\varepsilon} \tag{39}$$

Using (37), (38) and (39) a relation between damage increments and strain increments is obtained

$$\Delta \underline{D} = [P]^{-1}[Q]\Delta \underline{\varepsilon} \qquad if \ |\Delta \underline{X}| > 0 \wedge \phi_\alpha = 0 \tag{40}$$

with

$$\begin{aligned} P_{\alpha\beta} &= \delta_{\alpha\beta} + \left(\frac{\partial \phi_\alpha}{\partial \nu_\alpha}\right)^{-1} \left(\frac{\partial \phi_\alpha}{\partial X_\alpha}\right)^2 \frac{\partial X_\alpha}{\partial D_\beta} \\ Q_{\alpha j} &= -\left(\frac{\partial \phi_\alpha}{\partial \nu_\alpha}\right)^{-1} \left(\frac{\partial \phi_\alpha}{\partial X_\alpha}\right)^2 \frac{\partial X_\alpha}{\partial \varepsilon_j} \end{aligned} \tag{41}$$

The incremental change in the threshold parameter ν_α is found by substituting (40) in (37).

Tangential stiffness matrix

In the nonlinear range the stress increments can be expressed as

$$\Delta \underline{\sigma} = \frac{\partial \underline{\sigma}}{\partial \underline{D}} \Delta \underline{D} + \frac{\partial \underline{\sigma}}{\partial \underline{\varepsilon}} \Delta \underline{\varepsilon} = [V]\Delta \underline{D} + [C]\Delta \underline{\varepsilon} \tag{42}$$

The incremental change in the stiffness can be expressed in terms of the strain increments by substituting (41) in (42)

$$\Delta\underline{\sigma} = [C^{ED}]\,\Delta\underline{\varepsilon} \quad ; \quad [C^{ED}] = [C] + [V][P]^{-1}[Q] \tag{43}$$

where $[C^{ED}]$ is the elastic-damage tangential stiffness matrix. The evaluation of the components in $[C^{ED}]$ is discussed in Appendix I. Using (18) the matrices $[P]$ and $[Q]$ in (41) become

$$P_{ij} = \delta_{ij} - \frac{A_i}{X_0^i}\frac{\partial X_i}{\partial D_j} \quad ; \quad Q_{ij} = \frac{A_i}{X_0^i}\frac{\partial X_i}{\partial \varepsilon_j} \tag{44}$$

6. Examples

Uniaxial loading

Consider uniaxial loading of a graphite-epoxy AS4/3501-6 $[0/90_2]_s$ laminate. The stress state in the plies is assumed to be homogeneous. A simplified one-dimensional analysis is carried out together with a finite element analysis. The material data are given in Table 1. The strain at which damage growth in the 90° layer starts is $\varepsilon_0 = Y/E_T^0$ with Y the transverse tensile strength. It is assumed that damage propagation in the fiber mode is revealed as instantaneous laminate failure ($A_1 >> 1$). The associated strain is $\varepsilon_c = X/E_L^0$ with X the tensile strength. Using $A_2 = 1$, the maximum recorded transverse stress in the 90° layer can be derived as (Paas and van den Eikhoff 1992)

$$\breve{\sigma}_{22} = Y\sqrt{(D_2+1)\exp(-\gamma_{22}D_2)} \tag{45}$$

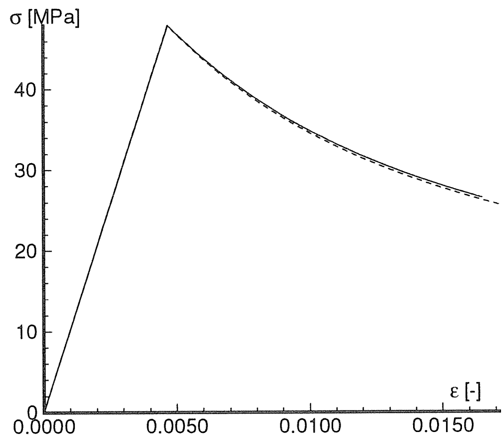

Fig. 1 Stress-strain relation for 90° ply in $[0/90_2]_s$ AS4/3501-6 laminate; --- analytical solution and —numerical solution.

Fig. 1 shows the stress-strain relation for the 90° ply. After the threshold ε_0 is exceeded, softening occurs. Fig. 2 shows the global stress versus D_2 according to the analytical solution and the finite element analysis. The finite element predictions and the analytical predictions almost coincide. The experimental results as reported by Lee and Daniel (1990) are also shown. Close agreement between experimental results and the calculated results is observed.

E_L [MPa]	E_T [MPa]	G_{LT} [MPa]	ν_{LT} [-]	Y [MPa]	X [MPa]	γ_{22} [-]	γ_{66} [-]
142000	10300	7600	0.3	51.7	1447	1.93	0.77

Table 1 Material Parameters for graphite-epoxy AS4/3501-6 (Lee and Daniel 1990, Tsai and Patterson 1990).

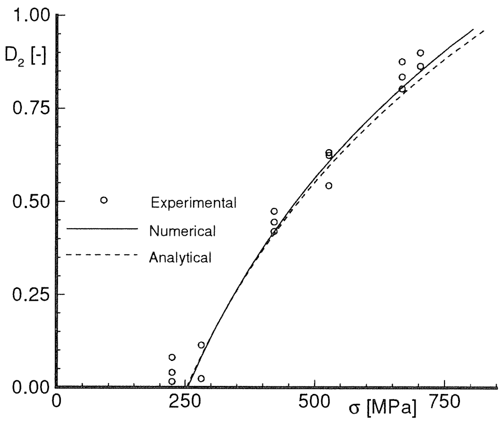

Fig. 2 Global stress versus D_2 for $[0/90_2]_s$ AS4/3501-6 laminate.

Bending

Consider a $[0/90_2]_s$ AS4/3501-6 graphite-epoxy laminated structure with dimensions 20*2*.75 mm^3. The structure is loaded at the right end by a vertical force F. The finite element discretization employed is given in Fig. 3. The material data are given in Table 1. The load-deflection curve is presented in Fig. 4. Some characteristic events in the failure process are marked A, B, C, D. At point A transverse cracks initiate in the 90° plies in the upper left element. A slight deflection of the slope of the stress-strain curve can be observed between A and B. At point B fiber fracture initiates in the upper left element. This event has significant influence on the stress-strain curve. At C a limit points is encountered. Beyond C softening occurs leading to rapid structural failure at point D.

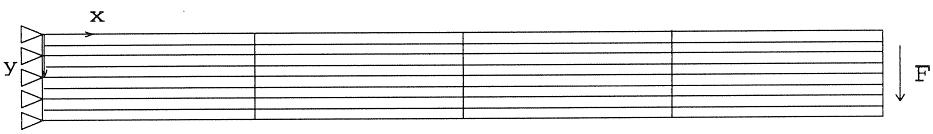

Fig. 3 Structure subjected to monotonic static loading.

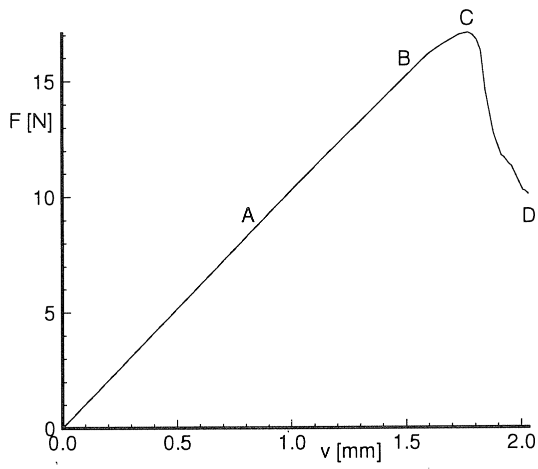

Fig. 4 Force vs. end displacement of $[0/90_2]_s$ AS4/3501-6 laminate.

Mesh sensitivity

The mesh sensitivity, which may occur in the post-critical region during brittle loading processes (Bazant 1986), is assessed for mesh refinement in both horizontal and vertical directions. The mesh sensitivity in the vertical direction was studied by keeping the number of elements over the length fixed and by varying the number of elements over the width. Finite element analyses were carried out with 8*4, 8*8 and 8*16 elements, respectively. Because structural softening is governed by fiber breaks (Fig. 4), the contribution of transverse cracking was omitted. Therefore, the analyses were carried out for one (unidirectional) ply only using the data in Table 1 (X = 1230 MPa). The computed load-deflection curves are presented in Fig. 5. The solutions show no mesh dependence for refinement in vertical direction. The mesh sensitivity in the horizontal direction was studied using 4*8, 8*8 and 16*8 elements, respectively. The computed load-deflection curves are shown in Fig. 6.

The solutions indicate that refinement in horizontal direction leads to zero energy dissipation for vanishing mesh size. The anisotropy in the mesh sensitivity is caused by the anisotropy in the damage, where fiber breaks govern the softening behavior.

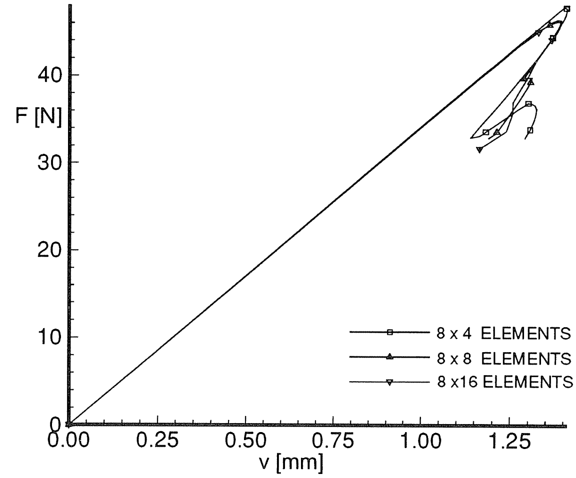

Fig. 5 Load vs end displacement for mesh-refinement in vertical direction.

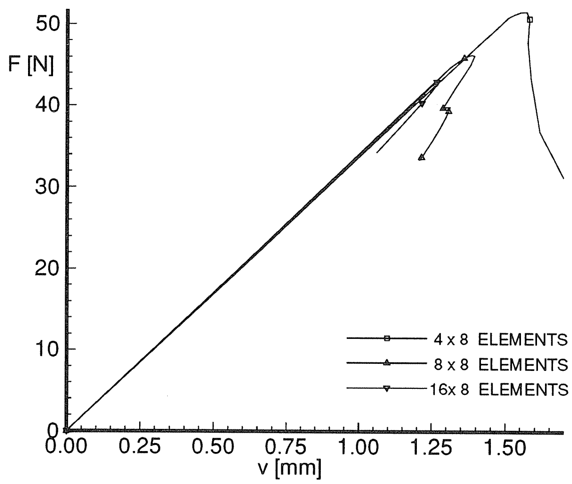

Fig. 6 Load vs end displacement for mesh-refinement in horizontal direction.

7. Discussion

An anisotropic damage theory was presented for brittle composite materials subjected to quasistatic loadings. The constitutive equations were derived on a thermodynamical basis. However, as far as matrix cracking is concerned, the stress-strain relation is inspired by micromechanics. The damage growth criterion yields quadratic criteria in stress space for both fiber fracture and matrix fracture.

The numerical procedures for solving the governing equations were discussed. To study the post-critical behavior it is essential to apply a method for arc-length control. The failure behavior of laminate structures was studied. Here a restriction was made to in-plane loading of symmetric laminates. For the uniaxial load case good correspondence with available experimental data was obtained. The mesh-sensitivity of the numerical simulations was investigated by comparing the solutions obtained upon mesh refinement. This was done in both horizontal and vertical directions. No mesh dependence was observed upon mesh-refinement in the vertical direction. Mesh refinement in horizontal direction led to solutions converging to a zero energy dissipation solution for vanishing mesh size, which is a physically unacceptable solution. However, this discussion is only relevant if, for the given load history and material, structural softening really occurs after having reached a limit point. The anisotropy in mesh sensitivity is caused by the anisotropy in the damage, where fiber breaks dictate the softening behavior. If softening occurs, the situation can be remedied by introducing a localization limiter associated with fiber failure, which prevents the structure from localization in an infinitely small region. This can be achieved in various manners (Sluys 1992). Introductory studies showed that the application of a local damage parameter in conjunction with a characteristic length for the cracked zone does reduce the mesh sensitivity and prevents the structure from failure with zero energy dissipation. The converged solution, however, does in general not coincide with the exact solution. Adopting a nonlocal damage model as proposed by Bazant and Pijaudier-Cabot (1988) is likely to provide better results. This topic is currently under research. Furthermore, future work will be directed toward the modeling of delaminations.

Acknowledgement

This work was sponsored by the Royal Dutch Navy. The authors gratefully acknowledge this financial support.

References

ALLIX, O. and LADEVEZE, P. (1989). A damage prediction method for composite structures. Int. J. Num. Meth. Engng., 27, pp. 271-283.

BATHE, K.J. (1982). Finite Element Procedures in Engineering Analysis. Prentice-Hall, Englewood Cliffs, New Jersey.

BAZANT, Z.P. (1986). Mechanics of distributed cracking. Appl. Mech. Rev., 39, pp. 675-705.

BAZANT, Z.P., and PIJAUDIER-CABOT, G. (1988). Nonlocal Continuum Damage, Localization Instability and Convergence. J. Appl. Mech., 55, pp. 287-293.

CHANG, K.Y., LIU, S. and CHANG, F.K. (1991). Damage tolerance of laminated composites containing an open hole and subjected to tensile loadings. J. Comp. Mater., 25, pp. 274-301.

CRISFIELD, M.A. (1991). Non-linear Finite Element Analysis of Solids and Structures, Vol 1. John Wiley & Sons, Chichester, England.

JONES, R.M. (1975). Mechanics of Composite Materials. Scripta Book Company, Washington, D.C..

KRAJCINOVIC, D. (1989). Damage Mechanics, Mech. Mater., 8, pp. 117-197.

LAWS, N., DVORAK, G.J., and HEJAZI, M. (1983). Stiffness changes in unidirectional composites caused by crack systems. Mech. Mater., 2, pp. 123-137.

LEE, J.W., and DANIEL, I.M. (1990). Progressive transverse cracking of cross-ply laminates. J. Comp. Mater., 24, pp. 1225-1243.

MALVERN, L.E. (1969). Introduction to the Mechanics of a Continuous Medium. Prentice-Hall, Englewood Cliffs, New Jersey.

NAHAS, M. N. (1986). Survey of failure and post failure theories of laminated fibre-reinforced composites. J. Comp. Tech. Res., 8, pp. 138-153.

PAAS, M.H.J.W., and EIKHOFF, J. VAN DEN (1992). An anisotropic damage model for brittle failure in laminated composite structures. TNO-report, nr. B-92-1139.

PAAS, M.H.J.W., and EIKHOFF, J. VAN DEN (1993). A continuum damage model for brittle deformation processes in fiber-reinforced composite materials. Submitted.

REIFSNIDER, K.L., and GIACCO, A. (1990). The use of microcrack analysis in performance simulation for composite material systems, in Microcracking-induced Damage in Composites. G.J. Dvorak and D.C. Lagoudas eds., ASME, pp. 19-27.

SLUYS, L.J. (1992) Wave Propagation, Localisation and Dispersion in Softening Solids. Ph. D. thesis Delft University of Technology, Delft, the Netherlands.

TALREJA, R. (1990). Internal variable damage mechanics of composite materials, in Yielding, Damage and Failure of Anisotropic Solids, EGF5. J. P. Boehler, ed., Mechanical Engineering Publications, London, pp 509-533.

TSAI, S.W. and PATTERSON, J.M. (1990). Design rules and techniques for composite materials, in Composite Materials in Aircraft Structures. Middleton, D.H. ed., Longman, Singapore.

WEITSMAN, Y. (1988a). Damage coupled with heat conduction in uniaxially reinforced composites. J. Appl. Mech., 55, pp. 641-647.

WEITSMAN, Y. (1988b). A continuum damage model for viscoelastic materials. J. Appl. Mech., 55, pp. 773-780.

Appendix I The elastic-damage tangent stiffness matrix

The evaluation of the components of the elastic-damage tangential stiffness matrix $[C^{ED}]$ is discussed in the following. In the materially nonlinear range the incremental stress-strain relation is

$$\Delta\underline{\sigma} = \frac{\partial\underline{\sigma}}{\partial\underline{D}}\Delta\underline{D} + \frac{\partial\underline{\sigma}}{\partial\underline{\varepsilon}}\Delta\underline{\varepsilon} = [V]\Delta\underline{D} + [C]\Delta\underline{\varepsilon} \tag{A.1}$$

This expression can be rewritten as

$$\Delta\sigma = [C^{ED}]\Delta\underline{\varepsilon} \;\; ; \;\; [C^{ED}] = [C] + [V][P]^{-1}[Q] \tag{A.2}$$

where $[C]$ is the current damaged material matrix. The components of $[V]$ follow from

$$V_{ij} = \frac{\partial \sigma_i}{\partial D_j} = \frac{\partial C_{ik}}{\partial D_j} \varepsilon_k \tag{A.3}$$

The components of $[P]$ and $[Q]$ are determined as

$$P_{\alpha\beta} = \delta_{\alpha\beta} + \left(\frac{\partial \phi_\alpha}{\partial \nu_\alpha}\right)^{-1} \left(\frac{\partial \phi_\alpha}{\partial X_\alpha}\right)^2 \frac{\partial X_\alpha}{\partial D_\beta} \quad ; \quad Q_{\alpha j} = -\left(\frac{\partial \phi_\alpha}{\partial \nu_\alpha}\right)^{-1} \left(\frac{\partial \phi_\alpha}{\partial X_\alpha}\right)^2 \frac{\partial X_\alpha}{\partial \varepsilon_j} \tag{A.4}$$

Starting point for the evaluation of the above matrices is the expression for the thermodynamic force

$$X_i = -\tfrac{1}{2} \varepsilon_k \frac{\partial C_{kl}}{\partial D_i} \varepsilon_l \tag{A.5}$$

From (A.5) we obtain

$$\frac{\partial X_i}{\partial \varepsilon_j} = -\frac{\partial C_{jk}}{\partial D_i} \varepsilon_k = -V_{ji} \tag{A.6}$$

$$\frac{\partial X_i}{\partial D_j} = -\tfrac{1}{2} \varepsilon_k \frac{\partial^2 C_{kl}}{\partial D_i \partial D_j} \varepsilon_l \tag{A.7}$$

The compliances S_{mn} are explicit functions of the damage parameters. Utilizing the identity

$$[C][S] = [I] \tag{A.8}$$

the first derivatives of the C_{kl} with respect to the damage parameters are

$$\frac{\partial C_{kl}}{\partial D_i} = -C_{km} \frac{\partial S_{mn}}{\partial D_i} C_{nl} \tag{A.9}$$

and the second derivatives are

$$\frac{\partial^2 C_{kl}}{\partial D_i \partial D_j} = -2 \frac{\partial C_{km}}{\partial D_j} \frac{\partial S_{mn}}{\partial D_i} C_{nl} - C_{km} \frac{\partial^2 S_{mn}}{\partial D_i \partial D_j} C_{nl} \tag{A.10}$$